Publications of the Korean Astronomical Society
30: 145 ∼ 148, 2015 September

pISSN: 1225-1534
eISSN: 2287-6936
http://dx.doi.org/10.5303/PKAS.2015.30.2.145

NEAR-INFRARED SPECTROSCOPY OF YOUNG GALACTIC SUPERNOVA REMNANTS

Bon-Chul Koo & Yong-Hyun Lee
Seoul National University, Seoul 151-747, Korea
E-mail: koo@astro.snu.ac.kr
(Received November 30, 2014; Reviced May 31, 2015; Aaccepted June 30, 2015)

ABSTRACT

Young Galactic supernova remnants (SNRs) are where we can observe closely supernova (SN) ejecta and their interaction with the circumstellar/interstellar medium. They also provide an opportunity to explore the explosion and the final stage of the evolution of massive stars. Near-infrared (NIR) emission lines in SNRs mostly originate from shocked dense material. In shocked SN ejecta, forbidden lines from heavy ions are prominent, while in shocked circumstellar/interstellar medium, [Fe II] and H_2 lines are prominent. [Fe II] lines are strong in both media, and therefore [Fe II] line images provide a good starting point for the NIR study of SNRs. There are about twenty SNRs detected in [Fe II] lines, some of which have been studied in NIR spectroscopy. We will review the NIR [Fe II] observations of SNRs and introduce our recent NIR spectroscopic study of the young core-collapse SNR Cas A where we detected strong [P II] lines.

Key words: infrared: ISM: shock waves: supernova remnants

1. INTRODUCTION

In the 1980s, NIR spectra of several SNRs were obtained (Seward, Harnden, Murdin, & Clark, 1983; Graham, Wright, & Longmore, 1987; Burton, Geballe, Brand, & Webster, 1988; Oliva, Moorwood, & Danziger, 1989; Graham, Wright, & Longmore, 1990; Oliva, Moorwood, & Danziger, 1990). A surprising result was that the forbidden lines of Fe II are much stronger than the hydrogen recombination lines, in contrast to HII regions. Also, it was found that NIR ro-vibrational H_2 lines are bright in some SNRs which might be interacting with molecular clouds (Burton, Brand, Geballe, & Webster, 1989; Burton & Spyromilio, 1993). These early studies showed that [Fe II] and H_2 lines are sensitive probes of shocked gas in SNRs.

More recently, it was found that the NIR spectra of young SNRs are interesting, sometimes showing many ionic lines from supernova (SN) ejecta material (Gerardy & Fesen, 2001; Koo et al., 2007; Moon et al., 2009; Lee et al., 2013; Koo et al., 2013). In the Milky Way, there are about 300 SNRs, and 20–30 of them are younger than several thousand years. These young SNRs still have the imprints of the explosion. So therefore, NIR spectroscopy can probe the explosion dynamics, SN nucleosynthesis, and the late-stage evolution of the progenitor star. Among young SNRs, G11.2−0.3, RCW 103, W49B, and Cas A are known to be bright in [Fe II] lines, and they are all small core-collapse SNRs that might be interacting with dense CSM (Koo, 2014). We have recently completed a survey of the Galactic plane in the [Fe II] 1.644 μm emission line, called UWIFE (UKIRT Widefield Infrared survey for Fe^+) survey (Lee et al., 2014a, see also the paper by Lee, J.-J. in this volume), where we detected [Fe II] emission in 17 out of 80 SNRs in the survey area ($\ell = 7^\circ$ to 65° and $|b| \leq 1.3^\circ$). Therefore, the sample of SNRs with [Fe II] emission will increase in the near future.

In this paper, we will first briefly summarize the characteristics and applications of NIR [Fe II] lines and then introduce our recent NIR spectroscopic study of Cas A where we detected strong [P II] lines.

2. NIR [Fe II] EMISSION FROM SNRs

[Fe II] line images of young SNRs show that [Fe II] line emitting regions are filamentary and spatially confined in contrast to radio or X-rays (see Fig. 4 of Koo, 2014).

This is because they originate from different environments. Figure 1 is a schematic diagram showing the structure of young SNRs. The SNR is bounded by a SN blast wave or forward shock. The shocked ambient medium is confined between the SN blast wave and a contact discontinuity. In the innermost region, there is freely expanding SN ejecta, which is heated when it encounters the reverse shock. Radio and X-rays are emitted from the shocked SN ejecta and shocked ambient medium, which is mostly circumstellar medium (CSM) in the case of young SNRs. In contrast, the NIR emission is emitted when the shocks encounter either dense ambient medium or dense SN ejecta and become radiative.

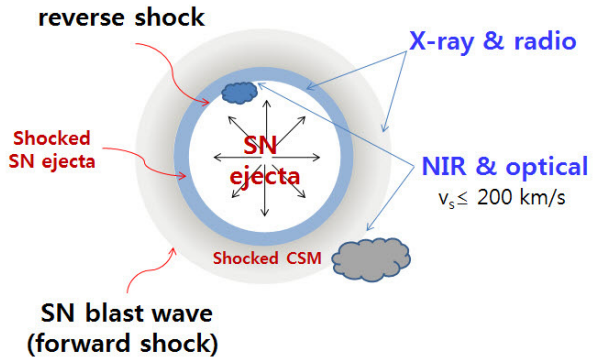

Figure 1. A schematic diagram showing the structure of young SNRs and where emission in different wavebands originates.

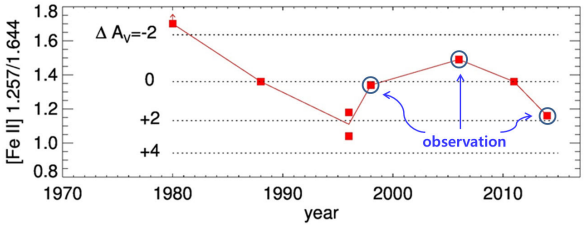

Figure 2. [Fe II] 1.257/[Fe II] 1.644 line intensity ratios reported in the literature. The dotted lines mark the differences in A_V when a [Fe II] 1.257/1.644 ratio different from 1.36 is adopted. References: Nussbaumer & Storey (1980), Nussbaumer & Storey (1988), Quinet et al. (1996) (SST/HFR), Bautista & Pradhan (1998) (observed, based on Everett & Bautista 1996 private comm.), Smith & Hartigan (2006), Deb & Hibbert (2011), Giannini et al. (2014)

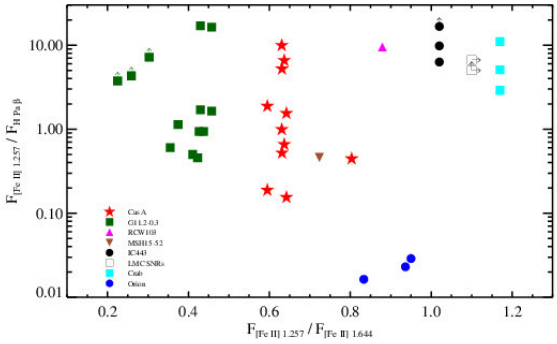

Figure 3. [Fe II] 1.257/H Pa-β versus [Fe II] 1.257/[Fe II] 1.644 line intensity ratio of SNRs. Note that the [Fe II] 1.257/[Fe II] 1.644 ratio is an indicator of extinction towards the source. The ratios of the Orion region are marked for comparison. Refereneces: Cas A (Gerardy & Fesen, 2001; Koo et al., 2013; Lee et al., 2014b), G11.2-0.3 (Koo et al., 2007; Moon et al., 2009), RCW 103 (Oliva, Moorwood, & Danziger, 1989, 1990), MSH 15-52 (Seward, Harnden, Murdin, & Clark, 1983), IC 443 (Graham, Wright, & Longmore, 1987), LMC SNRs (Oliva et al., 2001), Crab (Graham, Wright, & Longmore, 1990), Orion (Walmsley, Natta, Oliva, & Testi, 2000).

In shocks propagating into a medium of normal abundance, an extended temperature plateau region at $T_e \sim 10^4$ K develops in the postshock cooling region, and this is where the [Fe II] lines are emitted (Koo, 2014). In shocks propagating into SN ejecta, the temperature and emissivity profiles are very different because of strong cooling (Koo et al., 2013). Fe II has 16 levels near the ground state that can be easily excited in the cooling region, and can emit strong NIR lines. In the NIR band, the two strongest lines are the 1.257 and 1.644 μm lines, and 10–20 lines are seen (Koo, 2014, and references therein).

There are two direct applications of [Fe II] lines: (1) The extinction to the source can be accurately measured from lines originating from the same upper levels, and (2) the electron density of the emitting region can be derived using lines with comparable excitation energies. A major uncertainty in these applications is from atomic constants. For example, Figure 2 shows [Fe II] 1.257/[Fe II] 1.644 line intensity ratios, which are a good indicator of extinction, predicted by theoretical calculations and also the ratios derived from observations. There is still some scatter and, depending on which atomic constants you adopt, the value of A_V could be off by a few magnitudes.

As discussed earlier, the ratios of [Fe II] lines to H-recombination lines are much higher than those of HII regions, so this ratio can be used to discriminate the shock-ionized gas from photoionized gas. Figure 3 shows that the [Fe II] 1.257/H Pa-β line intensity ratio of SNRs is greater than 0.1 while it is 0.01–0.03 in the Orion HII region. The high ratio is partly due to the extended line-emitting region in the shock and probably also partly due to the increase of the gas-phase Fe abundance caused by the destruction of dust grains. For SNRs, one can derive the shock speed by comparing shock models. However, the predicted ratios can be different, sometimes by a large factor, so one should be careful when doing such analysis.

3. NIR [Fe II] AND [P II] EMISSION FROM Cas A

3.1. NIR Spectroscopy of Cas A

Cas A is a 330-yr old young SNR. It is one of the few SNRs whose SN type is confirmed from the spectra of light echos. It is a SN IIb with a progenitor mass between 15 and 25 $M_\odot$. Recently, IR space missions detected a significant amount of dust in this remnant, which increases the interest in this object.

From optical studies, it has been well known that there are two types of dense knots, namely FMKs, which are SN ejecta knots moving at several thousand km s^{-1} and QSFs which are dense CS knots moving at a few hundred km s^{-1}. A few people have carried out NIR spectroscopy to study the extinction to the remnant and also the density of knots (Gerardy & Fesen, 2001; Eriksen, Arnett, McCarthy, & Young, 2009). In particular, Gerardy & Fesen showed that the NIR spectral features

of FMKs and QSFs are quite different. We obtained JHK long-slit spectra along the bright shell and identified 63 clumps (Koo et al., 2013; Lee et al., 2014b). NIR spectra of the knots could be classified into three distinct groups: He-rich knots with strong He lines, S-rich knots with strong S and other intermediate mass element lines, and Fe-rich knots where essentially only Fe lines appear. These spectroscopically-distinct knots also demonstrate different kinematic properties. He-rich knots are moving slowly, while S-rich and Fe-rich knots are moving at velocities as high as 2000 km s^{-1}. These spectroscopic and kinematic properties imply that He-rich knots are CS knots corresponding to QSFs while S-rich knots are SN ejecta knots corresponding to FMKs. Fe-rich knots are most likely SN ejecta material from the innermost core.

3.2. [P II] lines in Cas A and SN Nucleosynthesis

Of the NIR lines, an interesting line is the 1.189 μm line of Phosphorus (P). It was detected mainly in S-rich knots and the line intensities were as strong as those of [Fe II] lines. This is surprising because P is not an abundant element. Its cosmic abundance is $X(\mathrm{P/H}) = 2.8 \times 10^{-7}$ and its relative abundance compared to Fe is only 1/110. The [P II] 1.189 μm line originates from a level whose excitation energy is almost identical to that of [Fe II] 1.257 μm line, and therefore the two lines originate from almost the same region in shocked gas. One can derive the relative abundance of the two elements directly from the line intensity ratios without a detailed analysis using a shock code. For the range of electron densities of the Cas A knots, i.e., $n_e = 3 \times 10^3$ to 2×10^5 cm^{-3}, $F_{[\mathrm{PII}]1.189}/F_{[\mathrm{FeII}]1.257} = (3-7)X(\mathrm{P/Fe})$ (Koo et al., 2013, see also Oliva et al. 2001). The derived X(P/H) of He-rich knots were close to solar abundance while the abundance of S-rich knots were as much as 100 times higher than the cosmic abundance. This confirmed the in situ production of P. The observed abundance ratios fit nicely into the theoretical range for 15 $M_\odot$SNs. However, the ratios were higher that the ratio for a complete mixing of the core below the He-rich layer, which implies that these dense knots largely retained their original abundances. This was the first result confirming the nucleosynthesis of P in SN.

3.3. [P II] lines for the ISM Study

The [P II] 1.189/[Fe II] 1.257 intensity ratio can be used for the study of shock processing of dust in the ISM because P is not depleted while Fe is mostly locked in dust grains. In the general ISM, therefore, the [P II] 1.189/[Fe II] 1.257 intensity ratio is high. However, in fast shocks, dust grains are destroyed, so that the gas phase Fe abundance increases and therefore the [P II]/[Fe II] ratio decreases. These properties have been used for the study of dust processing in HH objects and the origin of [Fe II] emission in external galaxies (e.g., Garcia Lopez et al., 2010; Oliva et al., 2001). Figure 4 shows $F_{[\mathrm{PII}]1.189}/F_{[\mathrm{FeII}]1.644}$ versus $F_{[\mathrm{FeII}]1.257}/F_{\mathrm{HPa}-\beta}$ for SNRs, HII regions, HH objects, and the galaxy NGC 1068. Note that both ratios are shock indicators, so that SNRs and HII regions are well separated in this diagram. NGC 1068, however, has a [P II] 1.189/[Fe II] 1.257 intensity ratio close to that of HII regions, but a [Fe II] 1.257/H Pa-β intensity ratio between those of HII regions and SNRs.

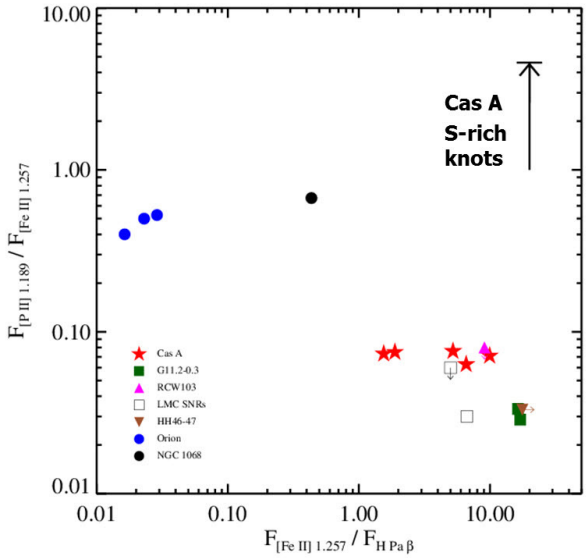

Figure 4. [P II] 1.189/[Fe II] 1.257 versus [Fe II] 1.257/H Pa-β line intensity ratios of various types of astronomical sources. Refereneces: Cas A Koo et al. (2013); Lee et al. (2014b), G11.2-0.3 (Moon, D.-S. personal communication), RCW 103 (Oliva, Moorwood, & Danziger, 1989, 1990), LMC SNRs (Oliva et al., 2001), HH46-47 (Garcia Lopez et al., 2010), Orion (Walmsley, Natta, Oliva, & Testi, 2000), and NGC 1068 (Oliva et al., 2001).

4. SUMMARY

The following is a brief summary:

(1) NIR spectra of SNRs are dominated by [Fe II] and H_2 emission lines unless the emission is from SN ejecta material. [Fe II] lines can be used to derive A_V, n_e, and shock parameters. However, there is an uncertainty associated with atomic parameters and shock codes. [Fe II] lines can be used to infer the environment of SNRs, e.g., the SNRs which are interacting with dense CSM are bright in [Fe II] lines.

(2) NIR spectroscopy of Cas A shows that CS and SN ejecta knots are clearly distinguished by their NIR spectra. [P II] lines are strong in S-rich SN ejecta material, and the derived X[P/Fe] is compatible with the local nucleosynthetic SN model. [P II] line provides an accurate X(P/Fe), which can be used to study the shock destruction of dust grains and the origin of [Fe II] emission lines.

ACKNOWLEDGMENTS

This research was supported by Basic Science Research Program through the National Research Foundation of Korea(NRF) funded by the Ministry of Science, ICT and future Planning (2014R1A2A2A01002811).

REFERENCES

Bautista, M. A., & Pradhan A. K., 1998, Ionization Structure and Spectra of Iron in Gaseous Nebulae and Partially Ionized Zones, Revista Mexicana de Astronomia y Astrofisica Conference Series, 7, 163

Burton, M. & Spyromilio, J., 1993, A Near Infrared View of Supernova Remnant / Molecular Cloud Interactions, Proceedings of the Astronomical Society of Australia, 10, 327

Burton, M. G., Brand, P. W. J. L., Geballe, T. R., & Webster, A. S., 1989, Molecular Hydrogen Line Ratios in Four Regions of Shock-excited Gas, MNRAS, 236, 409

Burton, M. G., Hough, J. H., Axon, D. J., Hasegawa, T., Tamura, M., McCaughrean, M. J., & McLean, I. S., 1988, Spectropolarimetry of the Molecular Hydrogen Line Emission from OMC-1, MNRA, 235, 161

Burton, M. G., Geballe, T. R., Brand, P. W. J. L., & Webster, A. S., 1988, Shocked Molecular Hydrogen in the Supernova Remnant IC 443, MNRAS 231, 617

Deb, N. C. & Hibbert, A., 2011, Radiative Transition Rates for the Forbidden Lines in Fe II, A&A, 536, AA74

Eriksen, K. A., Arnett, D., McCarthy, D. W., & Young, P., 2009, The Reddening Toward Cassiopeia A's Supernova: Constraining the 56Ni Yield, The Astrophysical Journal, 697, 29

Garcia Lopez, R., Nisini, B., Eislöffel, J., Giannini, T., Bacciotti, F., & Podio, L., 2010, IR Diagnostics of Embedded Jets: Kinematics and Physical Characteristics of the HH46-47 Jet, A&A, 511, AA5

Gerardy, C. L. & Fesen, R. A., 2001, Near-Infrared Spectroscopy of the Cassiopeia A and Kepler Supernova Remnants, AJ, 121, 2781

Graham, J. R., Wright, G. S., & Longmore, A. J., 1987, Infrared Spectroscopy of the Supernova Remnant IC 443, ApJ, 313, 847

Graham, J. R., Wright, G. S., & Longmore, A. J., 1990, Infrared Spectroscopy and Imaging of the Crab Nebula, ApJ, 352, 172

Giannini, T., Antoniucci, S., & Nisini, B., et al., 2014, Empirical Determination of Einstein A-coefficient Ratios of Bright [Fe II] Lines, ApJ, 798, 33, arXiv:1410.8304

Koo, B. -C., 2014, Infrared [Fe II] and Dust Emissions from Supernova Remnants, IAU Symposium, 296, 214

Koo, B. -C., Moon, D. -S., Lee, H. -G., Lee, J. -J., & Matthews, K., 2007, [Fe II] and H2 Filaments in the Supernova Remnant G11.2-0.3: Supernova Ejecta and Presupernova Circumstellar Wind, ApJ, 657, 308

Koo, B. -C., Lee, Y. -H., Moon, D. -S., Yoon, S. -C., & Raymond, J. C., 2013, Phosphorus in the Young Supernova Remnant Cassiopeia A, Science, 342, 1346

Lee, H. -G., and 11 colleagues, 2013, Wide Integral-field Infrared Spectroscopy of the Bright [Fe II] Shell in the Young Supernova Remnant G11.2-0.3, ApJ, 770, 143

Lee, J. -J., Koo, B. -C., & Lee, Y. -H., et al., 2014, UKIRT Widefield Infrared Survey for Fe+, MNRAS, 443, 2650

Lee, Y. -H., et al., 2014, in preparation

Moon, D. -S., Koo, B. -C., Lee, H. -G., Matthews, K., Lee, J. -J., Pyo, T. -S., Seok, J. Y., & Hayashi, M., 2009, Dense Iron Ejecta and Core-Collapse Supernova Explosion in the Young Supernova Remnant G11.2-0.3, ApJ, 703, L81

Nussbaumer, H. & Storey, P. J., 1980, Atomic Data for Fe II, A&A, 89, 308

Nussbaumer, H. & Storey, P. J., 1988, Transition Probabilities for Forbidden Fe II Infrared Lines, A&A, 193, 327

Oliva, E., Moorwood, A. F. M., & Danziger, I. J., 1989, Infrared Spectroscopy of Supernova Remnants, A&A, 214, 307

Oliva, E., Moorwood, A. F. M., & Danziger, I. J., 1990, Infrared Spectroscopy of Supernova Remnants. II - A Detailed Study of RCW 103, A&A, 240, 453

Oliva, E., and 21 colleagues, 2001, NICS-TNG Infrared Spectroscopy of NGC 1068: The First Extragalactic Measurement of [P II] and a New Tool to Constrain the Origin of [Fe II] Line Emission in Galaxies, A&A, 369, L5

Quinet, P., Le Dourneuf, M., & Zeippen, C. J., 1996, Atomic Data from the IRON Project. XIX. Radiative Transition Probabilities for Forbidden Lines in Fe II., A&AS, 120, 361

Seward, F. D., Harnden, F. R., Jr., Murdin, P., & Clark, D. H., 1983, MSH 15-52 - A Supernova Remnant Containing Two Compact X-ray Sources, ApJ, 267, 698

Smith, N. & Hartigan, P., 2006, Infrared [Fe II] Emission from P Cygni's Nebula: Atomic Data, Mass, Kinematics, and the 1600 AD Outburst, ApJ, 638, 1045

Walmsley, C. M., Natta, A., Oliva, E., & Testi, L., 2000, The Structure of the Orion Bar, A&A, 364, 301